

Characterization of an unusual carbon entity: 'gypsum flower'-like carbon

J. F. Despres,^a A. Genseki^b and O. Odawara^{a*}

^aDepartment of Electronic Chemistry, and

^bDepartment of Applied Electronics, Tokyo Institute of Technology, 4259 Nagatsuta Midori-ku, Yokohama 226, Japan

We present a description and a characterization of an unusual carbon entity which is produced in a combustion flame method. The process involved is very close to that of a diamond synthesis combustion flame and characterization is *via* electron microscopy (scanning and transmission). That carbon entity is revealed to be an sp² phase that presents a very unusual texture.

Compared to other techniques,¹ diamond films prepared by oxy-acetylenic flame combustion synthesis² are relatively inexpensive. Diamond-like and other carbonaceous species can also be produced³ by oxy-acetylenic flame combustion by varying the preparation and the source gases composition.⁵ Diamond films are composed of only sp³ bonded carbon while carbonaceous species are composed of sp² and sp³ bonded carbon. Since this growth technique involves processes very far from thermodynamic equilibrium, many uncertainties arise.⁴ This paper is focused on carbonaceous species, their textures (at the micro- and nano-scale) and their crystalline order. These species are then compared to pyrocarbons and soots obtained at similar temperature and pressure ranges under similar flame conditions to obtain more insight into the thermodynamic and kinetic processes controlling the structure of the deposited film.

Experimental

Experimental process

The preparation equipment details have previously been described.⁶ Note that the oxygen, acetylene and hydrogen source gases were metered using a commercially available mass flow meter system. The substrate was mounted on a temperature controlled water-cooled copper sample holder. Silicon substrates were used in all cases. The combustion flame deposition was carried out at ambient pressure. The O₂/C₂H₂ gas ratio used in this study was typically 0.90, with C₂H₂ and H₂ gas flows of 1.61 and 1.51 min⁻¹ respectively. During deposition the substrates were placed in the acetylene vertical flame feather zone (inner flame), 1 mm below the flame cone. The deposition time was held constant at 5 minutes for all cases. Substrate temperatures (*T_s*) ranged from 800 to 1250 °C (determined by IR pyrometry).

Characterization

All samples were characterized by scanning electron microscopy (SEM) and transmission electron microscopy (TEM). TEM samples were prepared by gently scraping the deposited film from the substrate. These free standing films were then fixed to an amorphous carbon coated metal grid for TEM analysis. All TEM modes (bright field, contrasted bright field, dark field and diffraction) were used.⁷ Selected area electron diffraction (SAD) was used to further probe the structure and crystalline order. Microtexture and anisotropy were determined by bright and dark field modes (BF and DF) whereas the nanotexture was analyzed using the fringes observed by high resolution electron microscopy (HREM). In the latter case the 002 fringes were obtained by imaging the

[001] aromatic layers which were oriented edge-on with respect to the grid surface.

Results and Discussion

Previously, Raman, SEM and X-ray diffraction studies established the qualitative relation between substrate temperature and structure. In this work we found at substrate temperatures ranging from 800 to 1050 °C, diamond or diamond-like films were obtained. At temperature > 1050 °C, an sp² carbon phase began to appear and at a temperature of 1250 °C Si-C and Si-O films were deposited. Nevertheless, multi-phase deposits were always obtained. Diamond and diamond-like species or diamond-like and sp² carbon species were identified in these deposits. Some films contained all three phases simultaneously. No precise deposition conditions could be found for each phase. Systematic variation of the deposition conditions revealed that while one phase would gradually diminish another would gradually increase. In particular in the temperature range 800–1050 °C, the percentage of diamond decreased with increasing temperature while the diamond-like content increased. At temperature above 1050 °C the diamond-like percentage decreased, while, the sp² percentage increased reaching a maximum at the highest temperature; these findings are in accord with the results of Bang *et al.*⁸ and Hanssen *et al.*³ Some unusual structures were found within the sp² phase at deposition temperatures of 1050–1250 °C.

The sp² phase coating appears matt black, similar to soots obtained by incomplete combustion of hydrocarbons. SEM studies revealed spherical bodies 5–10 μm in diameter (Fig. 1) with a very complex substructure shaped like a gypsum flower

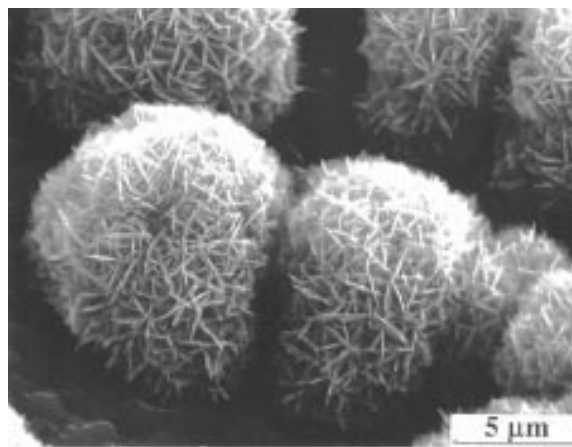


Fig. 1 SEM picture of 'gypsum flower'-like carbon (1200 °C)

(GF). This striking surface feature can be employed to define these sp^2 carbon structures. The size of the GF spheres, their compactness and the wall dimensions depend on the deposition temperature and/or on the local temperature within the sample. Fig. 2 shows a film prepared at 1200 °C where the GF spherical structures are clearly evident. The 'cooler' parts of the sample (furthest from the flame centre) show larger and more irregularly shaped GF spherical structures (Fig. 2), which resemble those seen by Balestrino *et al.*⁹ On the other hand, the hotter parts of the sample (near the flame center) exhibited much more regularly shaped features (Fig. 1). GF spherical structures are found both isolated (Fig. 1) and coalesced sufficiently to have the appearance of a continuous coating (Fig. 3).

Careful removal of the GF spherical structures containing layers could be easily accomplished using a scalpel and binocular microscope. The collected powder was then dispersed in ethanol. The suspension was then applied to the TEM grid and allowed to dry. Fig. 4 shows the walls of spherical structures (the global shape of GF spherical structures was too delicate to disturb without altering its shape). An aperture was used to block all scattered beams, including that from the sp^2 002 plane (contrasted bright field). Taking into account the different contrasts of the various areas, the lamellae appear to have a conical shape with folded edges as illustrated in the inset of Fig. 4. The SAD pattern of Fig. 5(a) was taken from one of these folded parts. This particular SAD pattern is that of pure sp^2 carbon where the aromatic layers are arranged on edge so that the pattern shows only the 002 reflections. There is a high degree of parallel stacking; patterns corresponding to 002 up to 006 are observed. In addition two maxima occur at the 101 reflection. The 101 peak is more intense than the 100 peak; this indicates three-dimensional ordering while the relative intensity of the 101 and 100 reflections indicates a high

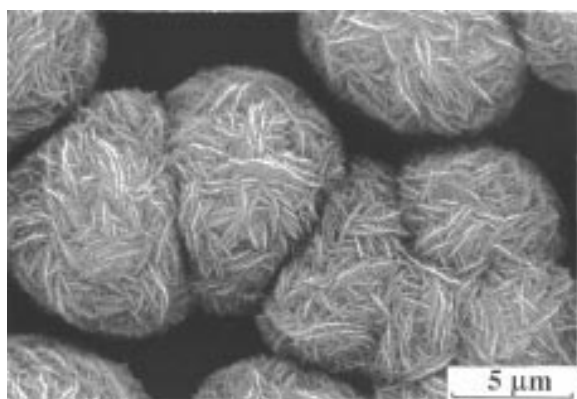


Fig. 2 SEM picture of GF morphologies in the cooler part of the substrate (1200 °C)

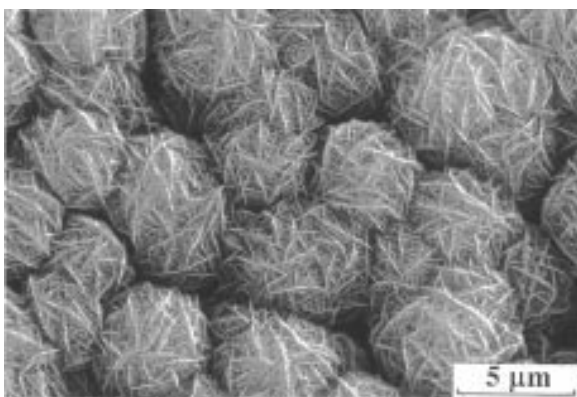


Fig. 3 SEM picture of a GF coating (1130 °C)

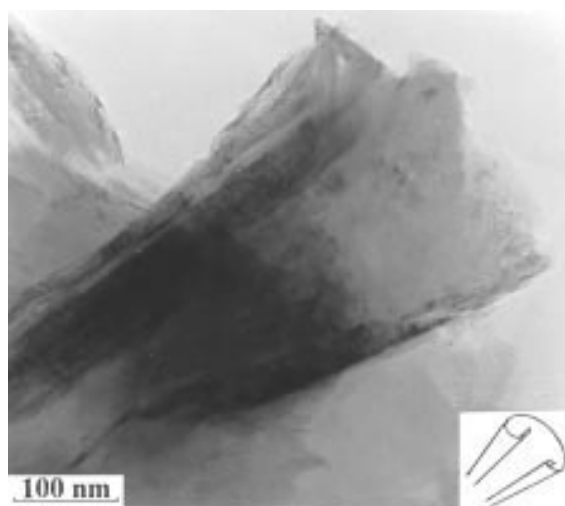


Fig. 4 BF mode picture of a wall (1130 °C)

level of graphitization (since 101 is more intense than the 100 reflection in the graphite structure). Interestingly thermally treated graphitizing carbons display the opposite intensity relation; that is, the reversal of the 100 and 101 intensities (at temperatures well above 2000 °C; 2450 °C is the value given by Monthieux *et al.*¹⁰). Fig. 5(b) shows the SAD pattern of the centre of the sample where the lamellae have pronounced curvature. This pattern corresponds to that of a powder pattern with a single hexagonal particle. The latter implies that the single crystal region has a diameter equal to or larger than that of the intermediate TEM aperture. The measurable diameters, were therefore limited to 0.6 μm. The powder pattern seen superimposed on that of the crystal pattern is due to tiny particles (also observed by SEM) distributed along the edge of external lamella walls. We assumed these were due to depositions occurring during the time in which the flame was extinguished.

A 110 dark-field TEM study was performed on one of the single crystal regions of the sample. Examining the rotational moirés patterns, we could determine the minimum size of coherent domains.⁷ Rotational moirés are typically produced by the random superposition of two coherent domains. These scattered beams interfere producing the moirés fringes. The length of the fringes is related to the size of the various superimposed domains. Therefore, it is possible to estimate the minimum size of the coherent domains. For the GF spherical structures ($T_s = 1130$ °C), the size of the coherent domain ranges from 50 to 100 nm.

In the HREM mode (Fig. 6) flat and straight fringes are observed. Negligible distortions are also seen in the TEM contrast. Such characteristics are typically seen in thermally treated graphitized carbons, prepared at temperatures >2000 °C. Therefore it is reasonable to assign a 2000 °C 'equivalent temperature' to the flame sample produced in this

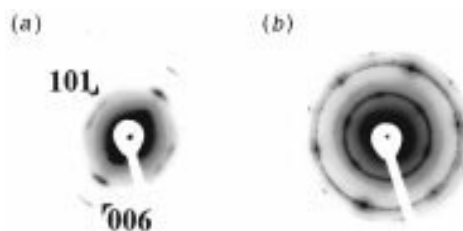


Fig. 5 SAD of (a) a turned up wall (1130 °C) and of (b) a flat wall (1130 °C)

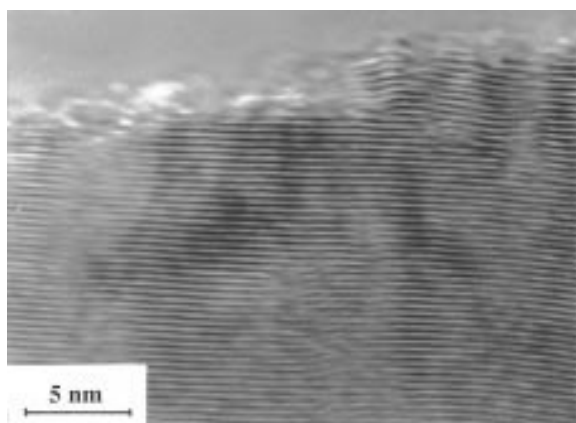


Fig. 6 HREM of a wall seen on the edge

work at $T_s = 1050^\circ\text{C}$. A more precise evaluation of the equivalent temperature can be established by considering the degree of graphitization¹¹ (P). Graphitization is a homogeneous process due to an increasing number of pairs of layers acquiring the atomic arrangement of the graphite. The value of P , equal to 1 for graphite, is related to the probability of finding graphite pairs of layers. However, knowing that these samples exhibit a 100 and 101 intensity reversal at *ca.* 2450°C (for $P = 0.76$), a more precise value of P can be estimated. The thickness of the GF walls, seen in the SEM micrographs, must be very thin ($< 50 \text{ \AA}$). In these lamella folds, the dark bands observed in the TEM bright field image (Fig. 4) or the bright bands observed in the 002 TEM dark field, are seen where the layer stacks are edge-on. The band widths are consistent with a minimum wall thickness of 20–25 nm ($T_s = 1130^\circ\text{C}$). Note these are minimum values since cleavages certainly occur during scratching of the deposit prior to TEM preparation.

A model for the sp^2 carbon bodies is shown in Fig. 7 where the GF spheres are defined by their overall size as well as the associated wall dimensions and structure (diameter and thickness of GF sphere, size of wall, diameter and thickness of coherent domain). It may also be interesting to define another parameter associated with the wall curvature, since, as in the case of nanotubes, curvature reflects wall stress.¹²

Conclusion

The GF-like particles observed here are entirely different from other flame products produced at similar temperatures. Low-temperature pyrocarbons (also produced within the range $1000\text{--}1200^\circ\text{C}$) or carbon blacks obtained from the gas phase have a completely different structure. These GF particles, although produced at a relatively low temperature, are almost totally composed of graphite, *i.e.* having very high three-dimensional ordered structure. In contrast pyrocarbons are able to graphitize but are turbostratic in the as-deposited state. Moreover, carbon blacks are poorly graphitizing even at very high heat treatment temperature (HTT) because of their small

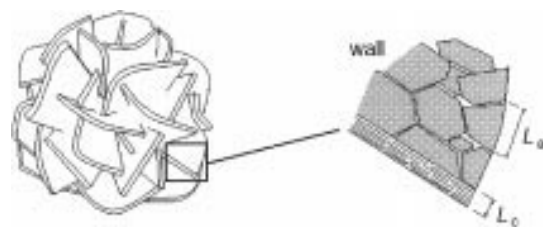


Fig. 7 Gypsum flower model and characteristic parameters

size. The maximum P value obtainable by heat treatment increases with particle diameter¹³ but never exceeds 0.4.¹⁴ In addition, the micro- and nano-texture of the carbonaceous GF bodies is radial with lamellae approaching those of low-temperature pyrocarbons¹⁵ whereas the carbon black structure shows a concentric texture.^{16,17} Since the products are so different in texture and structure, the GF-like growth may involve a different kinetic mechanism. Since it is found that chemical reactions occur in the silicon substrate, perhaps the substrate is also responsible for some of the observed effects at and above 1250°C . It is also plausible that the pre-deposit also influences the subsequent sp^2 growth kinetics where the complex reactions amongst carbon, silicon and oxygen (as proposed by Gulbransen and Jansson¹⁸ and Maniette and Oberlin¹⁹) influence the generation of the structures.

Finally, considering the sp^2/sp^3 phase diagram,^{4,17} it is surprising to find that the films prepared by the combustion flame method show no clearly defined growth regions where one phase is clearly favored over another. It is reasonable to expect that further study of these phase transitions will identify more favorable conditions for the production of diamond films from GF precursors.

References

- 1 K. V. Ravi, *Diamond Relat. Mater.*, 1995, **4**, 243.
- 2 Y. Hirose and K. Komaki, *Eur. Pat. Appl.*, EP 324538, 1988.
- 3 L. M. Hanssen *et al.*, *Thin Solid Films*, 1991, **196**, 271.
- 4 K. E. Spear, *J. Am. Ceram. Soc.*, 1989, **72**, 2, 171.
- 5 A. J. Ghajar and K. Bang, *Heat Transfer Eng.*, 1993, **14**, 3, 48.
- 6 H. Wada and O. Odawara, *J. Mater. Synth. Proc.*, 1993, **1**, 2.
- 7 A. Oberlin, *Chem. Phys. Carbon*, 1989, **22**.
- 8 K. Bang, A. J. Khajar and R. Komanduri, *Thin Solid Films*, 1994, **238**, 172.
- 9 G. Balestrino *et al.*, *Diamond Relat. Mater.*, 1993, **2**, 389.
- 10 M. Monthieux *et al.*, *Carbon*, 1982, **20**, 3, 167.
- 11 Warren, *Phys. Rev.*, 1941, **59**, 693.
- 12 J. F. Despres, E. Daguerre and K. Lafdi, *Carbon*, 1995, **33**, 87.
- 13 M. Inagaki and T. Noda, *Bull. Chem. Soc. Jpn.*, 1962, **35**, 1652.
- 14 N. Iwashita and M. Inagaki, *Carbon*, 1993, **31**, 1107.
- 15 J. F. Despres and A. Oberlin, *Tanso*, 1996, **171**, 2.
- 16 J. B. Donnet and Bouland, *Rev. Gen. Caoutch.*, 1964, **41**, 407.
- 17 R. D. Heindenreich, N. M. Hess and L. L. Ban, *J. Appl. Crystallogr.*, 1967, **1**, 1.
- 18 E. A. Gulbransen and S. V. Jansson, *Oxidation Met.*, 1972, **4**, 181.
- 19 Y. Maniette and A. Oberlin, *J. Mater. Sci.*, 1990, **25**, 3864.

Paper 7/01597F; Received 6th March, 1997